Available online at www.sciencedirect.com

ScienceDirect

journal homepage: www.elsevier.com/locate/he

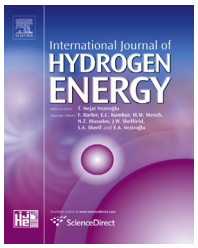

Glucose microfluidic fuel cell using air as oxidant

R.A. Escalona-Villalpando [a], A. Dector [b], D. Dector [a], A. Moreno-Zuria [a], S.M. Durón-Torres [c], M. Galván-Valencia [c], L.G. Arriaga [a], J. Ledesma-García [d,*]

[a] Centro de Investigación y Desarrollo Tecnológico en Electroquímica, 76703, Querétaro, Mexico
[b] Ingeniería en Tecnologías Industriales, Universidad Politécnica de Querétaro, 76240, El Marqués, Querétaro, Mexico
[c] Unidad Académica de Ciencias Químicas–Universidad Autónoma de Zacatecas, CU Siglo XXI, 96160, Zacatecas, Mexico
[d] División de Investigación y Posgrado, Facultad de Ingeniería, Universidad Autónoma de Querétaro, 76010, Santiago de Querétaro, Mexico

ARTICLE INFO

Article history:
Received 5 February 2015
Received in revised form
20 January 2016
Accepted 26 April 2016
Available online 16 June 2016

Keywords:
Air-breathing
Hybrid microfluidic fuel cell
Carbon nanotubes
Glucose oxidase enzyme
Glucose oxidation

ABSTRACT

A bioanode was constructed using glucose oxidase enzyme (GOx) supported on multi-walled–carbon nanotubes (MWCNTs) in the presence of glutaraldehyde (GA) (GOx/MWCNTs-GA) and evaluated in an air-breathing hybrid glucose microfluidic fuel cell (HG-μFC). The air-breathing HG-μFC operated under physiological conditions (5 mM glucose at pH 7 with an air-exposed cathode) delivers an open circuit value of 0.72 V with 610 μW cm^{-2} of maximum power density, and shows potential possibilities to develop future implantable applications.

Introduction

Glucose fuel cells (GFCs) are a type of conventional fuel cells that oxidize glucose in the anode and reduce oxygen in the cathode to generate electric energy. The GFCs, depending on the type of catalyst used, can be classified into different subtypes: abiotic, microbial and enzymatic [1]. Enzymatic glucose fuel cells (EGFCs) are attractive due to their high specificity for B-D-glucose, production of power densities in the order of several mW cm^{-2}, relatively inexpensive production and ability to work under conditions similar to physiological conditions (37 °C and pH 7) [2]. These qualities make them very effective for use in devices such as pacemakers, defibrillators, cochlear implants, neuro-stimulators, artificial hearts and drug delivery systems in living organisms [3]. However, EGFCs can produce low current density and power due to the poor stability associated with improper immobilization, inefficient electron conduction and the lifetime of the enzyme [4,5]. A few studies have already reported the use of an abiotic electrode (anode or cathode) in an enzymatic glucose fuel cell with the main target of providing stability and higher performance [6,38]. Thereby, hybrid glucose fuel cells

* Corresponding author.
E-mail address: janet.ledesma@uaq.mx (J. Ledesma-García).
http://dx.doi.org/10.1016/j.ijhydene.2016.04.238

(HGFC) represent an attractive alternative to be fabricated for these purposes [7]. Glucose oxidase (GOx) is the enzyme most employed as anode in EGFCs due to its stability, high catalytic activity and high selectivity toward glucose oxidation, as well as its low cost [8]. Many EGFCs that work involving GOx use PEMs (proton exchange membranes), which incorporate mediators to facilitate electron transfer from the enzyme to the electrode [9]. In this context, carbon nanotubes (CNTs) have been introduced to favour direct electron transfer because the specific nanowire morphology allows close interaction with the active site of the enzyme [10]. In addition, CNTs have unique properties such as high specific surface area, excellent biocompatibility, antifouling properties and high conductivity [11]. Furthermore, the PEM types of EGFCs are complexes and limit the possibility of micro fabrication; also, the PEM's membrane tends to swell, shrink and deform by drying or dehydration, resulting in operating inefficiencies [12]. Therefore, the replacement of PEM with co-laminar fluid flow in microfluidic fuel cells (μFCs) provides a viable alternative working towards miniaturized power devices with small power requirements [13]. Advantages of employing μFCs are the increased rates of mass transfer, less time consumption, reduced waste stream volume and problems related with the membrane [14]. Further advantage related to the use of liquid fuels is their higher volumetric energy densities compared to gaseous fuels [1,6].

In this work, one type of hybrid glucose microfluidic fuel cell (HG-μFC) that uses an exposed-abiotic cathode (air-breathing) and a bioanode prepared by cross-linking glucose oxidase enzyme (GOx) over multiwalled-carbon nanotubes (MWCNTs) was evaluated. The air-breathing HG-μFC was operated in the presence of 5 mM glucose (concentration close to that found in blood) in phosphate buffer pH 7 as anolyte, delivering an open circuit potential value (OCP) of 0.72 V and 610 μW cm^{-2} of maximum power density, which is a high value reported for this kind of device (Table 1).

Table 1 – Overview comparative of the HG-FC performances already reported.

Electron transfer anode	Anode (anolyte)	Cathode (catholyte)	OCV (V)	P_{max}/μWcm^{-2} (operating voltage)	Flow rate (μL min^{-1}	Fuel cell type	Reference
Anode: MET	GOx/CNT-GA (Glu 200 mM)	Pt (air-breathing)	0.33	120 (0.1 V)	68	PEM	[32]
Anode: MET	GOx/CNT-NF (Glu 100 mM/BQ 10 mM)	Pt-wire (O_2 gas)	0.57	77 (0.51 V)	1×10^5 (cathode)	PEM	[33]
Anode: MET	GOx/MWCNT-CS (Glu 3.8 M/FCHP)	Pt (gas diffusion electrode)	0.32	16 (0.2 V)	N.A	PEM	[34]
Anode: MET	GOx/Au-CS/DA (Glu 100 mM/BQ 4 mM)	Acidic $KMnO_4$	1.09	1600 (0.55 V)	N.S	PEM	[35]
Anode: MET	GOx-SF/CNT-Fc-GA (Glu 70 mM)	Pt-carbon (acetate buffer O^2 purging)	0.48	50.7 (0.15 V)	N.S	PEM	[36]
Anode: DET	GOx/CNT-GA (Glu 200 mM)	Pt-carbon (gas diffusion electrode 200 mM)	N.E	180	N.S	PEM	[37]
Anode: MET	GOx/CNT-GA (Glu 200 mM/10 mM BQ)	Pt (air-breathing)	0.51	250 (0.18)	N.A	PEM	[38]
Anode: MET	GOx/Maguemite (ϒ-Fe2O3)/Vulcan (Glu 10 mM)	Pt black (PBS O_2 purging)	0.30	30	21	Microfluidic	[39]
Anode: DET	GOx/MWCNT-GA (Glu 5 mM)	Pt/C (air-breathing)	0.72	610 (0.42)	8.33	Microfluidic	This work

MET: Mediated Electron Transfer, DET: Direct Electron Transfer, NF: Nafion; BQ: p-benzoquinone; PEGDGE: poly(ethyleneglycol) diglucidylether; CS: chitosan; Glu: glucose; N.A: not applicable; N.E: not specified; DA: dopamine; SF: silk film; Fc: ferrocenecarboxaldehyde; FCHP: ferroceniumhexafluorophosphate; TTF: tetrathiafulvalene; TCNQ: tetracyanoquinodimethane.

Experimental

Chemicals

Glucose oxidase enzyme (GOx) from Aspergillus Niger (100,000–120,000 U/g) type X-S, D-(+)-glucose ACS reagent and glutaraldehyde solution (GA) 50% were purchased from Sigma–Aldrich. KOH pellets (87%), H_2SO_4 (97.9%), HNO_3 (70%) and isopropyl alcohol were supplied by J. T. Baker. Nafion® 5% solution was acquired from Electrochem Inc. Phosphate buffer solution (PBS) was prepared by using Na_2HPO_4 and KH_2PO_4 from J. T. Baker. All aqueous solutions were prepared using deionized water ($\rho \geq 18$ MΩ cm).

Preparation of GOx/MWCNT-GA bioanode

For the half-cell experiments, a graphite surface (GP, dimensions 0.69 × 0.98 mm × 3 mm) was used as the working electrode. GP electrode was first polished with alumina (0.05 μm) until a mirror finish was obtained and then washed in an ultrasonic bath in acetone and deionized water for

20 min. After, the GP electrode was subjected to an electrochemical pre-treatment procedure by cycling in a solution of 0.5 M H_2SO_4 between −0.9 V and 1.3 V at 100 mV s^{-1}. Subsequently, the GP was washed with deionized water and dried at room temperature. On the other hand, MWCNTs were cleaned in 9 M HNO_3 at reflux for 24 h and dispersed in isopropyl alcohol (1 mg mL^{-1}) under ultrasonication for 1 h before being mixed with a solution of GOx-GA that was previously prepared by incorporating 5 mg mL^{-1} GOx in PBS pH 7 and 1% GA to immobilise via cross-linking. Finally, 50 μL of GOx/MWCNT-GA ink was deposited onto the GP surface and dried at room temperature.

Characterization and electrochemical measurements

The electrochemical tests in the half-cell consisted of cyclic voltammetry performed by potentiostat/galvanostat (BioLogic SAS Science Instrument VSP) in a standard three-electrode glass cell using a saturated calomel electrode (SCE) and Pt wire as the reference and counter electrode, respectively in N_2-saturated 0.1 mM PBS and room temperature. Additionally, Fourier Transform Infrared Spectroscopy-Attenuated Total Reflectance (FTIR-ATR) spectra were collected using a Perking Elmer FTIR spectrophotometer (Precisely Spectrum), in the spectral range of 600–4000 cm^{-1} for the ATR.

Hybrid glucose microfluidic fuel cell setup

The air-breathing HG-μFC consisted of one microchannel sandwiched between a pressure sensitive adhesive material and a piece of 20 micron-thick micro-porous Toray® carbon paper (Technoquip Co Inc TGPH-120) as the current collector (See Scheme 1). The fabrication was performed as follows: a silicone polymer film Silastic® (3-μm-thick) micromachined with a cutting plotter (Grapthec America Inc.) of 3.0 long × 1.0 cm wide and an opening of 0.1 × 0.9 cm was used as the microchannel. The anodic current collector was fabricated by using a material ARcare® 8890 (Adhesives Research Inc.) [6] covered by 0.66 cm^2 of adhesive graphite paper; meanwhile Toray® carbon paper (ElectroChem, Inc.) was used as the cathodic current collector. Dimensions of both current collectors were 3.0 × 1.0 cm wide with a central area of 0.95 × 0.47 cm where the catalyst was placed. The device was assembled for tests by aligning the three components and placing them between two polymethylmethacrylate PMMA pieces that were tightened by screws. In this case, the inlet solutions consisted of PBS (pH 7) and 5 mM glucose in N_2-saturated PBS for the cathodic and anodic compartment, respectively. The fuel cell tests were performed using a pressure driven fluid rate of 0.5 and 1.5 mL h^{-1} for the anolyte and catholyte, respectively. The flows were electronically controlled using a syringe pump (NE-400, New Era Pump Systems Inc.). The current and power

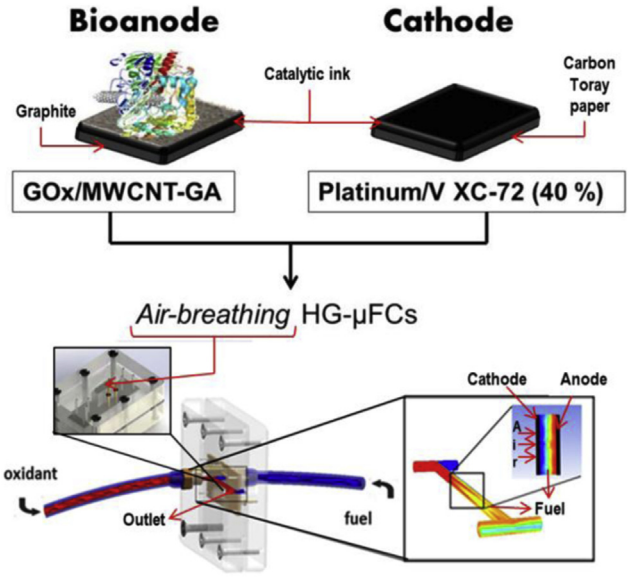

Scheme 1 – Schematic representation of the air-breathing hybrid glucose microfluidic fuel cell configuration.

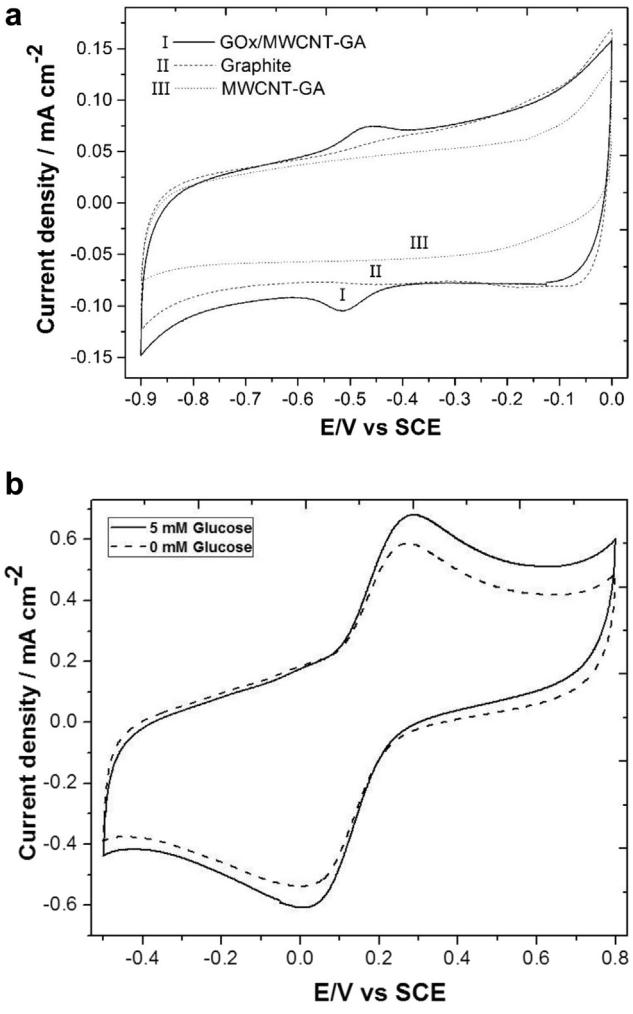

Fig. 1 – a) Cyclic voltammograms of GOx/MWCNT-GA on graphite (solid line) (I), Graphite (dashed line) (II) and MWCNT-GAon graphite (dot line) (III) in N_2-saturated 0.1 mM PBS. b) cyclicvoltammograms of 5 mM $K_4Fe(CN)_6$ at GOx/MWCNT-GA in N_2-saturated PBS pH 7 in the absence and presence of 5 mM glucose. Scan rate of 50 mV s^{-1} at room temperature.

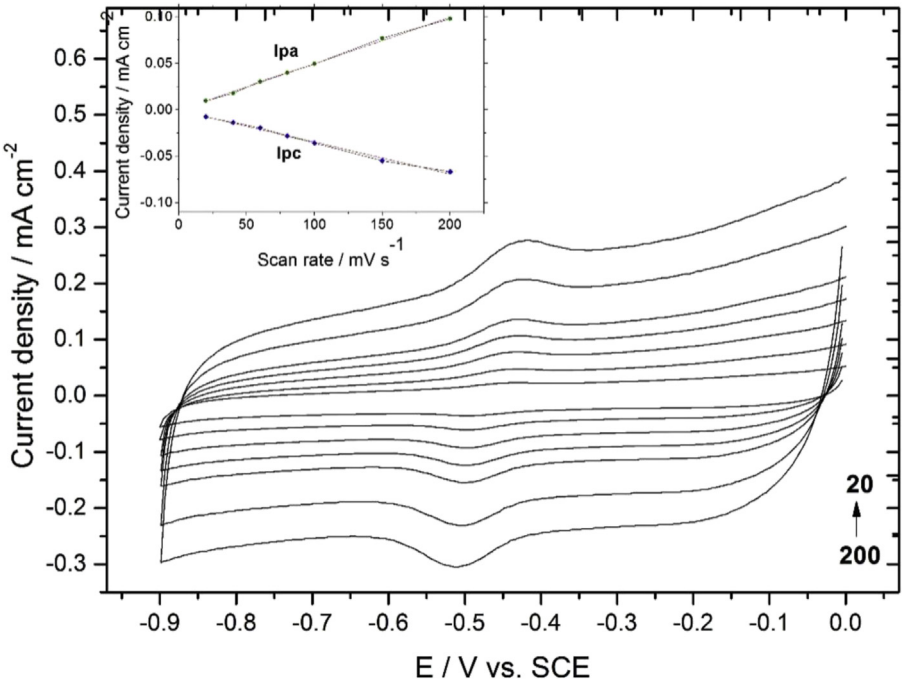

Fig. 2 – Cyclic voltammograms of GOx/MWCNT-GA on GP in PBS (pH 7) at different scan rates values. Plots of the anodic and cathodic current density *vs* the scan rate. Anodic lineal regression equation y = 0.00142x − 0.00687, r = 0.9989. Cathodic linear regression equation y = 0.00151x + 0.00301, r = 0.9998.

densities reported for this microfluidic fuel cell were calculated according to the planar active area of the electrodes in the microchannel (0.09 cm^2). The cathode was covered with a catalytic ink containing Pt/V XC-72 (40% from E-TEK) 7 μL of Nafion® (5% H_2O) and 73 μL of isopropyl alcohol, which was deposited by spray technique on the surface with a final metal loading of 1 mg cm^{-2} over the entire surface. In the bioanode, the GOx/MWCNT-GA catalyst was dropped on the surface.

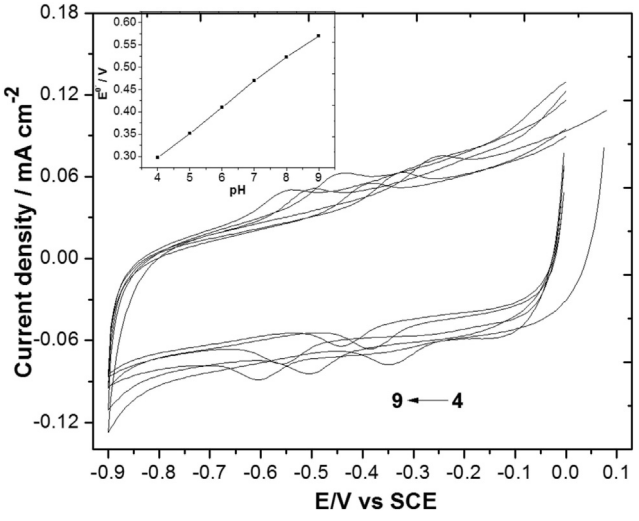

Fig. 3 – Cyclic voltammograms of the GOx/MWCNT-GA electrode in N_2-saturated 0.1 mM PBS at different pH values (4–9) with a scan rate of 50 mV s^{-1} and plot of formal potential value *vs*pH.

Results and discussion

Characterization of GOx/MWCNT-GA anode electrode

Fig. 1a compares the electrochemical responses of GP and GP modified with GOx/MWCNT-GA electrodes in PBS (pH 7), which exhibits a pair of anodic and cathodic peaks located at −0.46 and −0.505 V, respectively, which are attributed to the FAD/$FADH_2$ redox of the electroactive centre of GOx [16]. The difference of the potential peak of the process (ΔEp) is approximately 45 mV and a formal potential ($E^{0\prime}$) of 0.48 V vs. SCE; these values are similar to the pair of FAD/$FADH_2$ peaks already reported at pH 7.0 and 25.8 °C [17]. Both potential values suggested an efficient electron transfer between the GOx assisted by the MWCNTs on the GP surface [18].

Additionally, the surface coverage of the electroactive GOx on the GP was estimated according to the equation $\Gamma = Q/nFA$ [19] resulting in 2.15×10^{-10} mol cm^{-2}, where A is the apparent area of the electrode, *n* is the number of electrons transfer (equal to 2), *F* is Faraday's constant and Q is the amount of charge. The value of Γ shows high efficient coverage compared to theoretical value of 2.86×10^{-12} mol cm^{-2} for the GOx monolayer on the bare electrodes [20].

Furthermore, the electrocatalysis activity of GOx/MWCNT-GA was evaluated in N_2-saturated PBS solution pH 7 containing 5 mM $K_4Fe(CN)_6$ as redox mediator in the absence and presence of 5 mM glucose. In Fig. 1b well-defined redox peaks of $K_4Fe(CN)_6$ can be observed; however in the presence of glucose, the current density increases slightly suggesting that the enzyme is active [21].

Additionally, the effect of different scan rate values in an interval between 20 and 200 mV s^{-1} on GOx/MWCNT-GA on

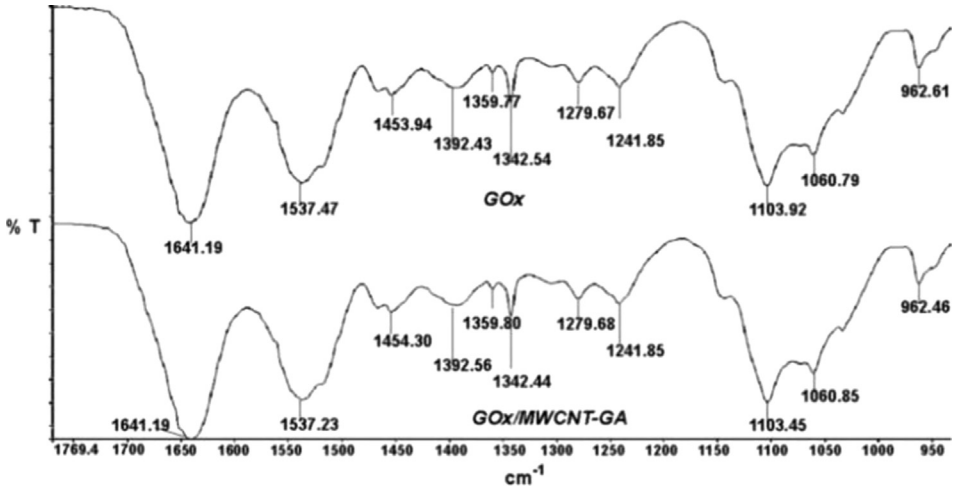

Fig. 4 – Fourier transforms infrared (FT-IR) spectra of pure GOx and GOx/MWCNT-GA mixture.

GP in PBS (pH 7) was tested (Fig. 2). A linear increasing of both anodic and cathodic peaks was observed as a function of the scan rate. This result indicates that the electron transfer process occurring at the GOx/MWCNT-GA film on the GP surface is controlled by an electrochemical process [22]. On the other hand, the electron transfer rate constant (Ks) for GOx/MWCNT-GA on GP was estimated according to the model of Laviron for a surface-control electrode process, considering a charge transfer coefficient of $\alpha = 0.5$ [23]. The obtained Ks value is 1.011 s^{-1} which is similar to values already reported using MWCNTs in enzymatic electrode arrangements [24,25].

It is well known that the electrochemical response of GOx immobilized on a surface is due to a redox reaction of FAD/$FADH_2$ bound to the enzyme, which transfers two electrons coupled with a two proton redox reaction [26]. Fig. 3 shows that an increase of the pH of the solution leads to a negative shift of potential for both anodic and cathodic peaks. The slope for a linear plot of $E^{0\prime}$vs pH is −55 mV pH^{-1} (r = 0.9983), which is close to the theoretical value of −58.6 mV pH^{-1} at 22 °C for a reversible system, indicating that two protons and two electrons participate in the electron transfer in the electrochemical reaction of GOx/MWCNT-GA immobilized onto the electrode carbon [27].

FTIR characterization of GOx/MWCNT-GA

Fourier transform infrared spectra at a range wave number 600 at 4000 cm^{-1} for GOx mixed with MWCNT-GA were recorded, analysed and compared with pure GOx. IR spectra for both are presented in Fig. 4. The FTIR spectra of pure GOx shows two characteristic absorption peaks at 1641 and 1537 cm^{-1} of the amides I and II, respectively. The peak observed at 1641 cm^{-1} is attributed to the C=O of the peptide linkage in the protein backbone, and the vibration at 1537 cm^{-1} is related to the combination of the N–H in plane bending and the C–N stretching of the peptide groups [28,29]. The FTIR spectra of GOx/MWCNT-GA show identical vibrations with respect to pure GOx indicating the presence of GOx in the MWCNT-GA mixture.

Performance of an air-breathing hybrid glucose microfluidic fuel cell

The polarization and power density curves of the air-breathing HG-μFC operates under physiological conditions pH 7 and 5 mmol L^{-1} glucose [30] are presented in Fig. 5 where an open circuit potential (OCP) of 0.72 V and a maximum power and current density of 610 μW cm^{-2} and 2.45 mA cm^{-2} respectively are observed. The polarization curve shows an increase in the ohmic loss and the variation of the cell potential corresponding to zero current. This phenomenon could be attributed to the effect of the availability of oxygen (0.2 cm^2 s^{-1} diffusion coefficient of oxygen in air) [15], delivery directly from air-exposed electrode in the cathode [31]. The performance of the HG-μFC that works with an air exposed-cathode achieved the highest value reported to date for hybrid glucose microfluidic fuel cells that use GOx/MWCNT. Additionally, an HG-μFC in a closed configuration (data not

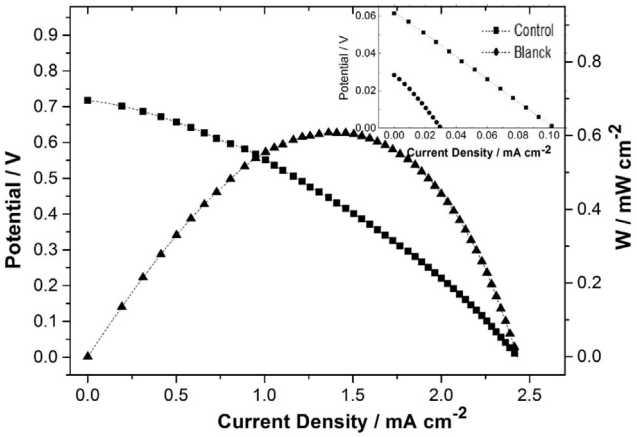

Fig. 5 – Polarization and power density curves of HG-μFC that uses glucose as fuel in N_2-saturated PBS and air-exposed cathode. Inset polarisation curves for control (no catalysts on the electrodes) and blank (no glucose in the solution).

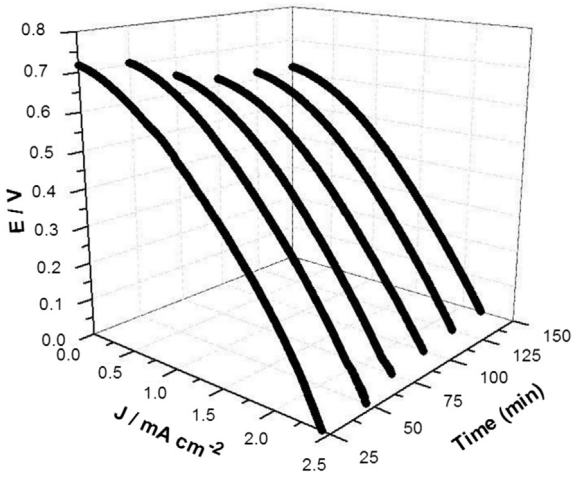

Fig. 6 – Stability curves of the air-breathing HG-μFC performed for 150 min of continuous operation (discharging the device each 25 min).

shown) operated under the same conditions, except the O_2-saturated catholyte, was evaluated as comparison. The closed device delivers the similar OCP value, but the maximum current and power density decreased around 50%. This result can be attributed to limited oxygen concentration in the cathode due to the oxygen diffusion coefficient in aqueous media (2×10^{-5} cm^2 s^{-1}) which is lower compared to that value in air [31].

Furthermore, the air-breathing HG-μFC was maintained under continuous operation for around 150 min, discharging the device each 25 min. Fig. 6 shows that the OCP value decreased from 0.72 V until 0.62 V, meanwhile the current density decreased to 2.25 mA cm^{-2} resulting in a final maximum power density value of 565 μW cm^{-2} after 150 min of continuous operation. This result is related with the capacity of the recovery and stability of the device.

Table 1 summarizes different types of HG-FC already described in the literature that have used GOx wiring MWCNTs in the anode and Pt in the cathode or abiotic and utilized mediator electron transfer. All of the devices are PEM type design but did not work under a microfluidic regime.

Finally, the fuel utilization (*FU*), which is defined as the current output divided by the flux of reactant entering the channel, is estimated by the following equation:

$$FU = \frac{1}{nFCQ}$$

where *n* is number of exchanged electrons, *F* is Faraday's constant, and *C* is the inlet concentration. 1.5%*FU* is obtained for the air-breathing HG-μFC at low flow rate (8.33 μL min^{-1}). According to Zebda et al. the typical fuel utilization for glucose microfluidic fuel cell is 1% when the device is operated from 100 to 1000 μL min^{-1}flow rate [40].

Conclusions

An enzymatic bioanode was constructed by means of immobilization of glucose oxidase enzyme on MWCNT in the presence of glutaraldehyde and evaluated toward glucose oxidation reaction in an air-breathing hybrid glucose microfluidic fuel cell. The comparative analysis of FTIR spectroscopy and electrochemical tests of pure GOx versus GOx-MWCNT-GA electrode confirms the presence of the GOx enzyme on the surface of the electrode. The performance of GOx/MWCNT-GA and Pt/C XC-72 as bioanode and cathode in the air-breathing HG-μFC evaluated under physiological conditions delivers an OCP of 0.72 V and a 610 μW cm^{-2} of maximum power density, which is the best result obtained to date for a glucose microfluidic fuel cell that uses an enzymatic anode and an air-exposed abiotic cathode. These results show the potential possibilities to develop future portable applications where it is necessary to use autonomous energy.

Acknowledgements

The authors thanks to Mexican Council for Science and Technology CONACYT for financial support through the Grants CB-2014-01-242787 and 611 Fronteras de la Ciencia.

REFERENCES

[1] Davis F, Higson SPJ. Biofuel cells—recent advances and applications. Biosens Bioelectron 2007;22:1224–35.
[2] Lapinsonnière L, Picot M, Barrière F. Enzymatic versus microbial bio-catalyzed electrodes in bio-electrochemical systems. ChemSusChem 2012;5:995–1005.
[3] Falk M, Blum Z, Shleev S. Direct electron transfer based enzymatic fuel cells. Electrochim Acta 2012;82:191–202.
[4] Brun N, Edembe L, Gounel S, Mano N, Titirici MM. Emulsion-templated macroporous carbons synthesized by hydrothermal carbonization and their application for the enzymatic oxidation of glucose. ChemSusChem 2013;6:701–10.
[5] Beneyton T, Mahendra IP, Salem CB, Griffiths AD, Taly V. Membraneless glucose/O2 microfluidic biofuel cells using covalently bound enzymes. Chem Commun 2013;49:1094–6.
[6] López-González B, Dector A, Cuevas-Muñiz FM, Arjona N, Cruz-Madrid C, Arana-Cuenca A, et al. Hybrid microfluidic fuel cell base don Laccase/C and AuAg/C electrodes. Biosens Bioelectron 2014;62:221–6.
[7] Zedba A, Tingry S, Innocent C, Cosnier S, Forano C, Moustry C. Hybrid layered double hydroxides-polypyrrole composites for construction of glucose/O2 biofuel cell. Electrochim Acta 2011;56:10378–84.
[8] Bankar SB, Bule MV, Singhal RS, Ananthanarayan L. Glucose oxidase – an overview. Biotechnol Adv 2009;27:489–501.
[9] Varfolomeev SD, Kurochkin IN, Yaropolov AI. Direct electron transfer effect biosensors. Biosens Bioelectron 1996;11:863–71.
[10] Zhang J, Feng M, Tachikawa H. Layer-by-layer fabrication and direct electrochemistry of glucose oxidase on single wall carbon nanotubes. Biosens Bioelectron 2007;22:3036–41.
[11] Holzinger M, Goff A, Cosnier S. Carbon nanotubes/enzyme biofuel cells. Electrochim Acta 2012;82:179–90.
[12] Mousavi SA, Nguyen NT, Chan SH. A review on membraneless laminar flow-based fuel cells. Int J Hydrogen Energy 2011;36:5675–94.

[13] ManoN Mao F, Heller A. A miniature membrane-less biofuel cell operating at +0.60 V under physiological conditions. ChemBioChem 2004;5:1703–5.
[14] Erickson D, Li D. Integrate microfluidic devices. Anal Chim Acta 2004;507:11–26.
[15] Patko D, Mártonfalvi Z, Kovacs B, Vonderviszt F, Kellermayer M, Horvath R. Microfluidic channels laser-cut in thin double-sided tapes: cost-effective biocompatible fluidics in minutes from design to final integration with optical biochips. Sens Actuator B Chem 2014;196:352–6.
[16] Hu F, Chen S, Wang C, Yuan R, Chai Y, Xiang Y, et al. ZnO nanoparticle and multiwalled carbon nanotubes for glucose oxidase direct electron transfer and electrocatalytic activity investigation. J Mol Catal B Enzym 2011;72:298–304.
[17] Oztekina Y, Ramanaviciene A, Yazicigil Z, Solak AO, Ramanavicius A. Direct electron transfer from glucose oxidase immobilized on polyphenanthroline-modified glassy carbon electrode. Biosens Bioelectron 2011;26:2541–6.
[18] Gao R, Zheng J. Amine-terminated ionic liquid functionalized carbon nanotube-gold nanoparticles for investigating the direct electron transfer of glucose oxidase. Electrochem Commun 2009;11:608–11.
[19] Wu P, Shao Q, Hu Y, Jin J, Yin Y, Zhang H, et al. Direct electrochemistry of glucose oxidase assembled on grapheme and application to glucose detection. Electrochim Acta 2010;55:8606–14.
[20] Xu JZ, Zhu JJ, Wu Q, Hu Z, Chen HY. Direct electron transfer between glucose oxidase and multi-walled carbon nanotubes. Chin J Chem 2013;21:1088–91.
[21] Lee SR,Lee YT, Sawada K, Takao H, Ishida M. Development of a disposable glucose biosensor using electroless-plated Au/Ni/copper low electrical resistance electrodes. Biosens Bioelectron 2008;24:410–4.
[22] Feng W, Ji P. Enzymes immobilized on carbon nanotubes. Biotechnol Adv 2011;29:889–95.
[23] Laviron E. General expression of the linear potential sweep voltammogram in the case of diffusionless electrochemical systems. J Electroanal Chem 1979;101:19–28.
[24] Cai C, Chen J. Direct electron transfer of glucose oxidase promoted by carbon nanotubes. Anal Biochem 2004;332:75–83.
[25] Periasamy AP, Chang YJ, Chen SM. Amperometric glucose sensor based on glucose oxidase immobilized on gelatin-multiwalled carbon nanotube modified glassy carbon electrode. Bioelectrochem 2011;80:114–20.
[26] Wong CM, Wong KH, Chen XD. Glucose oxidase: natural occurrence, function, properties and industrial applications. Appl Microbiol Biotechnol 2008;78:927–38.
[27] Wang K, Yang H, Zhu L, Ma Z, Xing S, Lv Q, et al. Direct electron transfer and electrocatalysis of glucose oxidase immobilized on glassy carbon electrode modified with nafion and mesoporous carbon FDU-15. Electrochim Acta 2009;54:4626–30.
[28] Haouz A, Twist C, Zentz C, Tauc P, Alpert B. Dynamic and structural properties of glucose oxidase enzyme. Eur Biophys J 1998;27:19–25.
[29] Zhao HZ, Sun JJ, Song J, Yang QZ. Direct electron transfer and conformational change of glucose oxidase on carbon nanotube-based electrodes. Carbon 2010;48:1508–14.
[30] Haghighi B, Tabrizi MA. Direct electron transfer from glucose oxidase immobilized on an over oxidized polypyrrole film decorated with Au nanoparticles. Colloid Surf B Biointerfaces 2013;103:566–71.
[31] Jayashree RS, Gancs L, Choban ER, Primak A, Natarajan D, Markoski LJ, et al. Air-breathing laminar flow-based microfluidic fuel cell. J Am Chem Soc 2005;127:16758–9.
[32] Fischback MB, Youn JK, Zhao X, Wang P, Park HG, Chang HN, et al. Electroanalysis 2006;18:2016–22.
[33] Zhao X, Jia H, Kim J, Wang P. Kinetic limitations of a bioelectrochemical electrode using carbon nanotube-attached glucose oxidase for biofuel cells. Biotechnol Bioeng 2009;104:1068–74.
[34] Buckner SW, Jelliss PA, Nukic A, Zalocusky ER, Schumacher J. A metallacarborane redox mediator for an enzyme-immobilized chitosan-modified bioanode. Bioelectrochem 2010;78:130–4.
[35] Chen C, Wang L, Tan Y, Qin C,Xie F, Fu Y, Xie QJ, et al. High-performance amperometric biosensors and biofuel cell based on chitosan-strengthened cast thin films of chemically synthesized catecholamine polymers with glucose oxidase effectively entrapped. Biosens Bioelectron 2011;26:2311–6.
[36] Liu J, Zhang X, Panga H, Liu B, Zou Q, Chen J. High-performance bioanode based on the composite of CNTs-immobilized mediator and silk film-immobilized glucose oxidase for glucose/O2 biofuel cells. Biosens Bioelectron 2010;3:170–5.
[37] Dudzik J, Chang WC, Kannan WAM, Filipek S, Viswanathan S, Li P, et al. Cross-linked glucose oxidase clusters for biofuel cell anode catalysts. Biofabrication 2013;5:1–9.
[38] Fischback M, Kwon KY, Lee I, Shin SJ, Park HG, Kim BC, et al. Enzyme precipitate coatings of glucose oxidase onto carbon paper for biofuel cell applications. Biotechnol Bioeng 2012;109:318–24.
[39] Galindo R, Dector A, Arriaga LG, Gutiérrez S, Herrasti P. Maghemite as a catalyst for glucose oxidation in a microfluidic fuel cell. J Electroanal Chem 2012;671:38–43.
[40] Zebda A, Gondran C, Goff AL, Holzinger M, Cinquin P, Cosnier S. Mediatorless high-power glucose biofuel cells based on compressed carbon nanotube-enzyme electrodes. Nat Commun 2011;2:1–6.